

## RF DESIGN OF AN X-BAND TM<sub>02</sub> MODE CAVITY FOR FIELD EMITTER TESTING\*

Z. Li<sup>#</sup>, S. G. Tantawi, SLAC National Accelerator Laboratory, Menlo Park, USA.  
T. Y. Posos, M. S. Schneider, S. V. Baryshev, Michigan State University, East Lansing, USA.

### Abstract

Planar polycrystalline synthetic diamond with nitrogen-doping/incorporation was found to be a remarkable field emitter. It is capable of generating a high charge beam and handling moderate vacuum conditions. Integrating it with an efficient RF cavity could therefore provide a compact electron source for RF injectors. Understanding the performance metrics of the emitter in RF fields is essential toward developing such a device. We investigated a test setup of the field emitter at the X-band frequency. The setup included an X-band cavity operating at the TM<sub>02</sub> mode. The field emitter material will be plated on the tip of an insertion rod on the cavity back plate. Part of the back plate and the emitter rod are demountable, allowing for exchange of the field emitters. The TM<sub>02</sub> mode was chosen such that the design of the demountable back plate does not induce field enhancement at the installation gap. The cavity was optimized to achieve a high surface field at the emitter tip and a maximum energy gain of the emitted electrons at a given input power. We will present the RF and mechanical design of such a TM<sub>02</sub> X-band cavity for field emitter testing.

### INTRODUCTION

Nitrogen-incorporated ultrananocrystalline diamond (N-UNCD) films have been shown to be an excellent field emitter with a low turn-on surface field and a stable emission current [1-4]. The planar (N)UNCD cathodes have been tested and shown to perform in both normal and superconducting environments, and in DC and RF fields. Hence, it may be of use in both normal and SRF linac systems. Unlike legacy field emission electron sources consist of Spindt-type arrays of nanometer-size high aspect-ratio tips, the N-UNCD can be a thin film synthesized on a substrate material without needing of complicated processes such as lithography. Moreover, the N-UNCD can be grown directly onto any refractory metal. So that the field emitter based on the N-UNCD can be made into a variety of shapes and sizes. It provides flexibilities in the emitter design to optimize the emission current and beam characteristics. It potentially capable of generating a high charge beam, ~1-10 pC per RF cycle, and handling moderate vacuum conditions and can be refurbished [5]. Integrating it with an efficient RF cavity could therefore provide a compact electron source for RF injectors. Such electron sources, if validated, could significantly benefit the system design of

a wide range of accelerator applications. For example, this would eliminate the high voltage elements in a compact accelerator application thus greatly reduce the size and weight of the system; the source produces bunched electrons thus eliminates the bunching elements and associated beam loss heating. The N-UNCD emitter has the potential to reach ultralow emittance and energy spread due to intrinsic properties [6] and via various gating methods [7, 8]. Experiments have shown emission at field levels of 1 MV/m and up. The full operational range, from turn-on up to the breakdown field, must be explored systematically before N-UNCD can be considered for accelerator applications. Understanding the performance metrics of the emitter in RF fields in miniature high frequency environment is essential. Maintaining high field emission cathode performance over long-term operation remains an important goal to realize high-performance field emission electron source-based injectors. Toward this goal, we investigated a test setup of the field emitter at the X-band frequency. The setup included an X-band cavity operating at the TM<sub>02</sub> mode. The field emitter material will be plated onto the tip of an insertion rod on the cavity back plate. Part of the back-plate and the emitter rod are demountable, allowing for exchange of the field emitters. Mechanically, the cavity body and the demountable back plate are brazed onto a standard 2.75" flange. An insertion hole is machined out on the flange that is brazed on the cavity. A large cylinder piece is brazed onto the other side of the flange and is inserted into the hole to form part of the cavity back wall. This insertion may leave with a coaxial gap on the back wall of the cavity, by design or by the tolerance of a tight fit. This can induce field enhancement and potentially causing multipacting in the gap. To mitigate these issues, the TM<sub>02</sub> mode was chosen such that the design of the demountable back-plate does not induce field enhancement at the insertion gap and the field in the gap is suppressed by design to eliminate the multipacting. The cavity was optimized to achieve a high surface field at the emitter tip and a maximum energy gain of the emitted electrons at a given input power. This paper presents the RF and mechanical design of such a TM<sub>02</sub> X-band cavity.

### CAVITY RF AND MECHANICAL DESIGN

The cavity geometry is required to accommodate the flexibility of a demountable back-plate so that different emitters can be tested or swapped at the end of their lifetime with ease. The field emission material is plated onto the tip of a cylinder rod. The rod is intruded into the cavity to produce a high electric field enhancement at the tip. The tip is rounded to obtain a uniform field distribution in a large portion of the hemispheric surface. The emitter rod is

\*Work at SLAC was supported by DOE under contract No. DE-AC02-76SF00515. Work at MSU was supported by DOE under Award No. DE-SC0020429 and under Cooperative Agreement Award No. DE-SC0018362.

<sup>#</sup>lizh@slac.stanford.edu

Content from this work may be used under the terms of the CC BY 3.0 licence (© 2021). Any distribution of this work must maintain attribution to the author(s), title of the work, publisher, and DOI

screwed on to the back-plate. The demountable back-plate is flush with the back wall of the cavity. The field emission electrons are emitted at the peak of the electric field with virtually zero velocities. The phase of these electrons would slip away from the peak phase quickly as they are being accelerated toward the beam exit. Both the tip length and the acceleration gap should be optimized to maximize the field enhancement and acceleration to minimize the power requirement. To calculate the power requirement for a given tip field, we define a “point shunt impedance R” as Eq. (1),

$$\left(\frac{\text{point}R}{Q}\right) = \frac{E_{cat}^2}{\omega U} \quad (1)$$

With this definition, the power for a given tip field can be calculated by Eq. (2).

$$\text{Power} = \frac{E_{cat}^2}{\left(\frac{\text{point}R}{Q}\right) Q_0 \frac{4\beta}{(1+\beta)^2}} \quad (2)$$

### Cavity Shape Comparison

Initially, both the TM01 and TM02 mode cavities were considered. We finally settled on the TM02 cavity design for the test stand. Figure 1 shows the E and B field distribution of the TM01 and TM02 modes. The acceleration gap is defined as the distance from the tip to the front face of the beam port. The tip length and the gap are optimized to minimize the RF power requirement. The nominal operation electric field at the tip is 120 MV/m. Figure 2 shows the comparison of the RF parameters of these two cavity shapes vs the tip length and gap.

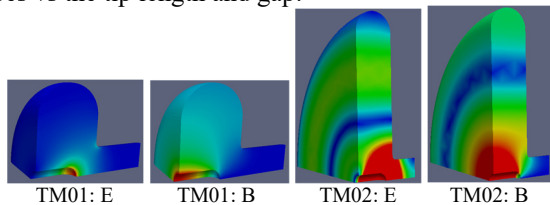


Figure 1: Operating mode of TM01 and TM02 mode cavities.

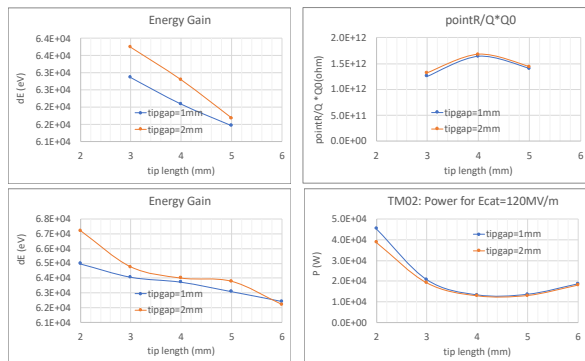


Figure 2: RF parameter comparison between TM01 mode (top) and TM02 mode (bottom) cavities.

Generally, the pointR and the power requirement are at their optimal around a tip length of about 4 mm. The energy

gain of both cavities is above 60 keV, which is well in the range of injection energy for many accelerator applications [9-12]. This energy gain is not very sensitive to the gap size (1mm vs. 2mm). The TM01 cavity is more efficient and requires about 40% less RF power. This is mainly due to a higher  $Q_0$  of the TM01 mode. However, this advantage in a TM01 mode cavity is largely diminished as the demountable back-plate feature is included. In the TM01 cavity, the gap of the demountable back-plate would be at a region of higher magnetic field which could result in a significant reduction in  $Q_0$ .

### The TM02 Mode Cavity

The cavity design will utilize standard 2.75” and 1.33” CF flanges to mount both the cavity body and the emitter back-plate, as shown in Fig. 3. The flange on the cavity side is cut through allowing the back-plate mounted on the other side of the flange to plug in. There is a 0.2 mm gap between the black-plate plug and the plug hole, which forms a coaxial volume. The depth of this coaxial volume is determined by the half thickness of the flange, which is 12.7 mm. This coaxial gap can potentially couple to the cavity RF field causing reduction in  $Q_0$ . Fig. 4 shows the effect of this coaxial coupling to the TM02 mode and the TM01 mode. With a properly chosen gap radius, this coupling in the TM02 mode design can be totally rejected. While in the TM01 mode design, this coupling always existed which caused a significant  $Q_0$  reduction. The TM02 mode cavity turned out to be a better choice to achieve the design objective of this test setup. The rounding at the outer perimeter of the cavity improves the cavity  $Q_0$ . However, the mechanical design adopted a simple pillbox shape geometry for ease of machining. The full summary of the RF parameters of the TM02 cavity is given in Table 1.

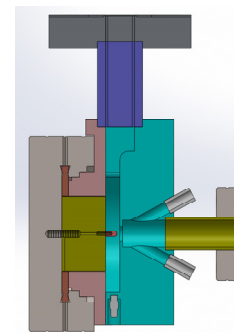


Figure 3: A side cutaway view of the full mechanical gun assembly.

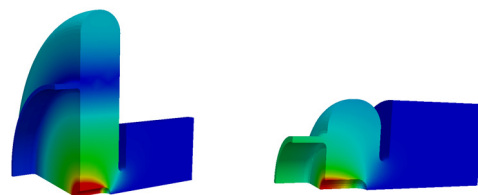


Figure 4: The magnetic field contour plots to illustrate the coupling of the modes to the plug gap. The TM02 mode cavity (left) is chosen as it totally rejects this coupling. In

the TM01 design (right), the insertion gap exposes to a strong magnetic field which results in a strong coupling.

Table 1: TM02 Mode Cavity Parameters

Parameter	Value	Unit
Mode type	TM02	
Frequency	11.424	GHz
Quality factor $Q_0$	5300	
(point Shunt impedance) pointR/Q	195	$M\Omega$
Emitter tip electric field	120	MV/m
RF coupling beta	1.05	
RF power required	13.3	kW
Beam energy	63	kV
Bunch charge	1	pC
Cavity length	5	mm
Beam iris aperture	4	mm
Beam port radius	4.875	mm
Emitter tip radius	1	mm
Emitter tip length	4	mm
Emitter gap	1	mm
Back plug gap	0.2	mm
Back plug length	13.7	mm

### POWER COUPLER

The power coupling is through a typical longitudinal slot at the outer diameter of the cavity. The coupling port starts with a reduced WR90 waveguide height to match to the cavity length. It then steps up to the full WR90 via a quarter wave transformer, which enhanced the coupling and in turn reduced azimuthal opening of the slot. The coupling beta is 1.05 to achieve a critical coupling with a small beam loading due to the field emitted current at a tip electric field of 120 MV/m. The coupling port is one-sided. This naturally induces a field asymmetry in the cavity. It is desirable to minimize the effect of this field asymmetry because of the low beam energy in the cavity. Field symmetrisation is incorporated into the design by shifting the cavity volume 0.09 mm off the field emitter (and beam axis) axis as shown in Fig.5. The two plots on the right of Fig. 5 show the on-axis transverse magnetic field, before and after the symmetrisation. A factor of 20 reduction is achieved.

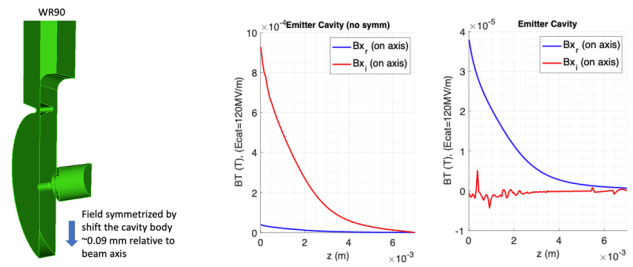


Figure 5: Power coupler and the result of field symmetrisation.

### FIELD IN THE BACK-PLATE GAP

One of the major concerns with a narrow gap in an RF cavity is the multipacting. In the TM02 cavity design, the radial position of the gap is chosen to minimize its coupling to the RF field. Figure 6 shows the electric and magnetic fields inside the gap. The gap extends from  $z=0$  to  $z=0.013$  m. The fields in the plots are normalized, by the field solver, to a  $E_{max}$  of  $1.14e4$  MV/m. Scaled to the design emitter surface field of 120 MV/m, the electric field in the gap is about 0.5 MV/m and the magnetic field is about  $9e-4$  T respectively. For multipacting to exist in the gap, the energy of the electrons accelerated across the gap need to be in the range that has a secondary yield greater than 1. At this electric field level, the maximum energy gain for an electron is less than 100 eV when accelerated across the gap. The secondary yield for a copper surface typically peaks at around 600-700 eV. The electron impact energy in the gap is well below this range. Multipacting is thus not considered an issue. Furthermore, tight fit plug design is also considered should multipacting become problematic. Additional RF loss in the gap is minimal and does not cause any  $Q_0$  reduction.

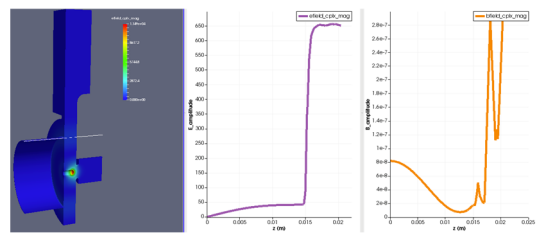


Figure 6: E and B field distribution in the gap ( $z=0$  to  $z=0.013$ m).  $E_{max} < 0.5$  MV/m;  $B_{max} < 9e-4$ T at a tip E field of 120 MV/m.

Both the RF and mechanical designs of the TM02 cavity have been completed. Particle-in-cell simulation of field emission is being carried out and is to be benchmarked with the experiment.

## REFERENCES

- [1] J. Qiu *et al.*, “Nanodiamond Thin Film Field Emitter Cartridge for Miniature High-Gradient Radio Frequency X-Band Electron Injector”, in *IEEE Transactions on Electron Devices*, vol. 65, no. 3, pp. 1132-1138, Mar. 2018. doi:10.1109/ted.2017.2788822
- [2] S. V. Baryshev *et al.*, “Planar ultrananocrystalline diamond field emitter in accelerator radio frequency electron injector: Performance metrics”, *Appl. Phys. Lett.*, vol. 105, p. 203505, Nov. 2014. doi:10.1063/1.4901723
- [3] S. V. Baryshev *et al.*, “Cryogenic operation of planar ultrananocrystalline diamond field emission source in SRF injector”, *Appl. Phys. Lett.*, vol. 118, p. 053505, Feb. 2021. doi:10.1063/5.0013172
- [4] J. Shao *et al.*, “High power conditioning and benchmarking of planar nitrogen-incorporated ultrananocrystalline diamond field emission electron source”, *Phys. Rev. Accel. Beams*, vol. 22, p. 123402, Dec. 2019. doi:10.1103/physrevaccelbeams.22.123402
- [5] M. Schneider *et al.*, “Ampere-class bright field emission cathode operated at 100 MV/m”, Jan. 2021. arXiv:2102.00071
- [6] T. Nikhar *et al.*, “Evidence for Anti-Dowell-Schmerge Process in Photoemission from Diamond”, Nov. 2020. arXiv:2011.00722
- [7] X. Li *et al.*, “Cold cathode RF guns based study on field emission”, *Phys. Rev. Spec. Top. Accel. Beams*, vol. 16, p. 123401, Dec. 2013. doi:10.1103/physrevstab.16.123401
- [8] J. W. Lewellen and J. Noonan, “Field-emission cathode gating for rf electron gun”, *Phys. Rev. Spec. Top. Accel. Beams*, vol. 8, p. 033502, Mar. 2005. doi:10.1103/physrevstab.8.033502
- [9] S. Tantawi *et al.*, “Design and demonstration of a distributed-coupling linear accelerator structure”, *Phys. Rev. Accel. Beams*, vol. 23, p. 092001, Sep. 2020. doi:10.1103/physrevaccelbeams.23.092001
- [10] S. G. Tantawi *et al.*, “Distributed coupling and multifrequency microwave accelerators”, U.S. Patent No. 9386682 Jul. 05, 2016. <https://www.osti.gov/servlets/purl/1260195>
- [11] SLAC – The future of fighting cancer: zapping tumors in less than a second, <https://www6.slac.stanford.edu/news/2018-11-28-future-fighting-cancer-zapping-tumors-less-second.aspx>
- [12] P. G. Maxim *et al.*, “PHASER: A platform for clinical translation of FLASH cancer radiotherapy”, *Radiother. Oncol.*, vol. 139, pp. 28-33, Oct. 2019. doi:10.1016/j.radonc.2019.05.005